

Sorption of Np(V), Pu(V), and Pu(IV) on Colloids of Fe(III) Oxides and Hydrrous Oxides and MnO₂

A. B. Khasanova^a, N. S. Shcherbina^a, S. N. Kalmykov^a,
Yu. A. Teterin^b, and A. P. Novikov^c

^a Chemistry Faculty, Lomonosov State University, Moscow, Russia

^b Russian Research Centre Kurchatov Institute, Moscow, Russia

^c Vernadsky Institute of Geochemistry and Analytical Chemistry, Russian Academy of Sciences, Moscow, Russia

Received March 20, 2006

Abstract—Sorption of Np(V), Pu(V), and Pu(IV) on colloids of synthetic goethite (α -FeOOH), hematite (α -Fe₂O₃), maghemite (γ -Fe₂O₃), and amorphous MnO₂ was studied over wide ranges of solution pH and ionic strength by solvent extraction and X-ray photoelectron spectroscopy (XPS). Plutonium(V) is reduced upon sorption on α -FeOOH, but not on α -Fe₂O₃ and γ -Fe₂O₃. On the MnO₂ surface, Pu occurs as Pu(VI). From the pH dependences of the actinide sorption, the equilibrium constants of the reactions of Np(V)O₂⁺ and Pu(V)O₂⁺ with the surface hydroxy groups of the investigated colloid particles and a set of the equilibrium constants of the reactions of Pu(IV) hydroxo complexes with α -FeOOH were obtained. If no redox reactions occur on the surface of the colloid particles, these constants decrease in the order $K_{\text{MnO}_2} > K_{\alpha\text{-FeOOH}} > K_{\alpha\text{-Fe}_2\text{O}_3} \sim K_{\gamma\text{-Fe}_2\text{O}_3}$.

PACS numbers: 68.43.-h, 82.70.Dd, 89.60.Ec

DOI: 10.1134/S1066362207040170

The modern approaches to long-term safety assessment of radioactive waste (RW) repositories in surface and underground geological formations are based on data on the radionuclide sorption on components of engineered and geochemical barriers (rocks and minerals), and also on the solubility of radionuclides in underground waters. Repositories for RW should meet the criterion that radionuclides from RW must not enter the human habitation zone in tens and hundreds thousand years. According to most of the existing estimates, tri- and tetravalent actinides and Tc(IV) represent no hazard, as having strong tendency to sorption on components of engineered barriers and host rocks and also as having extremely low solubility. However, recent data suggest the possibility of colloidal migration of these radionuclides in groundwater [1–6]. Kersting et al. [7] reported that, at the test site in Nevada, ²³⁹Pu was carried with smectite colloid to a distance of 1.3 km in 30 years. Penrose et al. [8] have studied the behavior of Pu and Am in the Mortandad canyon (Los Alamos National Laboratory) and found that these radionuclides have migrated with colloid particles to a distance of 3390 m from the source. By the way, the theoretical estimates for the migration rates of these radionuclides suggested that their path is limited to several meters. It was

demonstrated by the methods of micro- and ultrafiltration that Pu and Am are associated with colloid particles 25–450 and ≤ 2 nm in size, respectively. However, no information on the nature of these colloids was reported.

Naturally occurring minerals differ considerably in their sorption capacity for cations, and the available data on the preferential sorption of radionuclides on colloid particles of various kinds are contradictory. Duff et al. [9] studied the Pu sorption on tuff with inclusions of zeolite, smectite, and Fe and Mn oxides by various microanalytical methods. They have demonstrated that Pu is sorbed on smectites and Mn oxides only, and in the latter case, it is oxidized to Pu(VI).

A great deal of work has been made to model radionuclide sorption on various minerals, including oxides and hydrrous oxides of Fe [10–12] and Mn [13–15], clay [16], calcite [15], etc. Most authors employ the distribution coefficient K_d as a parameter characterizing the sorption. However, the use of this parameter is limited to specific experimental conditions (pH, complexation, etc.). An alternative approach to description of the sorption involves calculation of the equilibrium constants of one or another sorption reaction occurring on the surface of colloid

Table 1. Characteristics of colloid samples

Parameter	α -FeOOH	α -Fe ₂ O ₃	γ -Fe ₂ O ₃	MnO ₂
Total specific surface area, m ² /g*	41.7	6.4	20.4	182
Specific micropore surface area, m ² /g*	7.23	3.02	9.8	32.9
Mean particle size, μ m**	0.30 \pm 0.05	0.35 \pm 0.05	–	–
pH(IEP) ***	8.8	9.4	8.9	1.5

* From BET analysis.

** From SEM data.

*** From potentiometric titration data.

particles. From the set of the equilibrium constants of all possible reactions occurring both in solution and on the surface of colloid particles, one may estimate K_d for any system.

This study is aimed to examine the sorption of Np(V), Pu(V), and Pu(IV) on various Fe(III) oxides and hydrous oxides and MnO₂, to determine the valence states of the actinides, and to estimate the equilibrium constants for sorption reactions. Colloidal iron and manganese oxides and hydrous oxides may be formed under conditions of both near-by and distant zones of RW repositories, representing a factor strongly influencing the behavior of radionuclides. Furthermore, such iron oxides as hematite (α -Fe₂O₃) and magnetite (α -Fe₃O₄) can be formed in contour water of nuclear reactors under the action of water radiolysis products [17]. Transformation of magnetite to hematite and sorption of radionuclides are the factors determining to a considerable extent the decision on the methods for contour water management. As mentioned above, a great body of information is gained on the radionuclide sorption on Fe and Mn oxides and hydrous oxides. However, data on the equilibrium constants of sorption reactions are either lacking at all or contradictory [9, 14, 16, 18].

EXPERIMENTAL

Preparation and Characterization of Colloid Particles of Fe(III) and Mn(IV) Oxides and Hydrous Oxides

Colloidal goethite (α -FeOOH) was synthesized by the procedure described in [19]. A weighed portion of Fe(NO₃)₃·9H₂O was dissolved in deionized water, 2.5 M KOH was added to pH 12, and the reaction mixture was vigorously stirred for 24 h at 60°C. The resulting suspension was dialyzed until the total nitrate concentration in the outer solution was $<10^{-4}$ M. Finally, the colloid suspension was multiply washed with acetone and dried at 40°C for 48 h.

Colloidal hematite (α -Fe₂O₃) was synthesized according to [20]. A weighed portion of FeCl₃·6H₂O

was dissolved in deionized water, concentrated HCl was added to pH 1.5, and the solution was heated to 100°C. The resulting hot solution was diluted with the estimated volume of hot deionized water, placed in a Teflon vessel, and heated in a pressure vessel at 90–100°C for a week. After cooling, the suspension was separated by centrifugation, multiply washed with double-distilled water, and air-dried at 80°C.

Colloidal maghemite (γ -Fe₂O₃) was synthesized by the method described in [21]. A weighed portion of FeCl₃·6H₂O was dissolved in deionized water, 2.5 M NaOH was added, and the mixture was heated at 70°C for 2 days. Then the mixture was heated in a pressure vessel at 350°C for 1 h. The suspension was separated by centrifugation, multiply washed with double-distilled water, and dried.

Colloidal manganese dioxide was synthesized by the method described in [22]. To a solution of KMnO₄ in NaOH, MnCl₂ was added stepwise with magnetic stirring. The resulting suspension was settled for 24 h, filtered off, multiply washed with deionized water, and air-dried.

The samples were characterized by X-ray diffraction (XRD), scanning electron microscopy (SEM), and potentiometric titration [21]. The BET surface area was determined from the nitrogen adsorption. No foreign phases were found in Fe-containing samples. Manganese dioxide samples are amorphous. Characteristics of the samples are summarized in Table 1.

Aqueous solutions for the sorption experiments were prepared with deionized water (Milli-Q) treated to remove CO₂ by purging ultrapure grade N₂. Solution pH values were measured with a combined glass electrode [Mettler Toledo InLab (Switzerland)].

Preparation and Purification of Pu(IV), Pu(V), and Np(V)

Since the Pu sorption experiments were planned to carry out at various total Pu concentrations, Pu iso-

topes of different specific activity were used (^{242}Pu , ^{239}Pu , and ^{238}Pu). The radioactivity of solutions was measured using liquid scintillation spectrometry (TriCarb 2700TR, Packard Ind.).

Plutonium in the oxidation state 4+ was stabilized by adding a small amount of NaNO_2 to the stock nitric acid solution [23] and was monitored by the UV spectra (Shimadzu UV-3100).

Solutions of Pu(V) were prepared by electrolytic method [23]. The completeness of Pu(IV) oxidation to Pu(V) was controlled by the UV spectra. Just prior to the sorption experiments, the Pu(V) solution was treated with 0.05 M HDEHP (Merck) in heptane to remove traces of Pu(IV) and Pu(VI) formed through disproportionation of Pu(V) [24].

Purification of ^{237}Np to remove the daughter ^{233}Pa was performed by adding 0.5 M TTA (Lancaster) in cyclohexane to the stock Np solution in 1 M HNO_3 . The oxidation state of Np was monitored by the UV spectra.

Sorption Experiment

To eliminate the sorption of the actinides on the walls and carbonate complexation, the sorption experiments were carried out in plastic vials (20 and 50 ml in volume) under nitrogen atmosphere. All the experiments were performed at $25 \pm 2^\circ\text{C}$. Goethite, hematite, maghemite, and manganese dioxide were used as colloidal suspensions at concentrations of 0.36, 0.44, 0.38, and 0.30 g l^{-1} , respectively. The supporting electrolyte was 0.001–0.1 M NaClO_4 . After adding the colloid to an actinide-containing solution, the desired pH was adjusted with dilute NaOH or HClO_4 . After sorption, the liquid phase was separated by filtration through a 170-nm filter, and its radioactivity was measured. The sorption efficiency was estimated from the difference between the radionuclide concentrations in the initial solution and filtrate.

Pu and Np Redox Speciation

The actinide redox speciation on the colloid surface was studied using solvent extraction with TTA and HDEHP after desorption of the radionuclides with 1 M HClO_4 according to the scheme presented in Fig. 1 [14]. Since the redox speciation of the actinides can change during the desorption and solvent extraction stages, the samples containing microgram amounts of Pu and Np occurring initially as Pu(V) and Np(V) were examined by XPS. The XPS spectra were re-

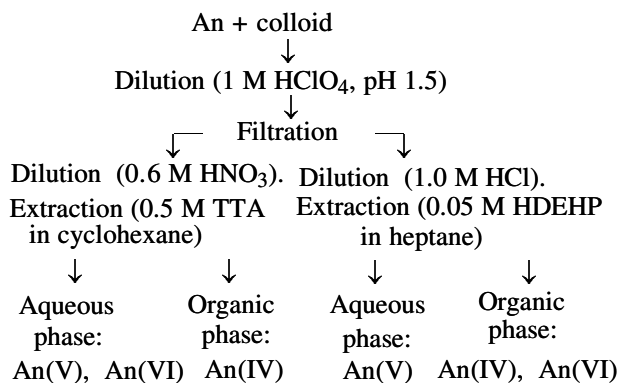


Fig. 1. Flowsheet of extraction separation of actinides to study their redox speciation.

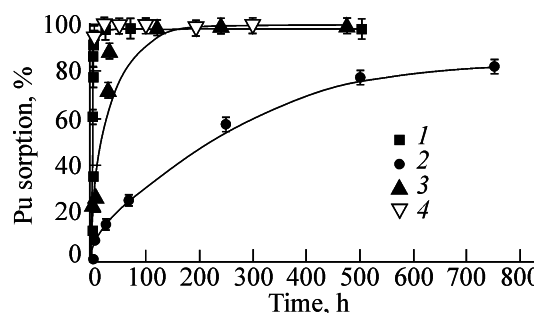


Fig. 2. Sorption kinetics from Pu(V) solution [$c(\text{Pu}) = 10^{-8}$ – 10^{-9} M, $c(\text{NaClO}_4) = 0.1$ M] on (1) $\alpha\text{-FeOOH}$ ($15 \text{ m}^2 \text{ l}^{-1}$), pH 5.5; (2) $\alpha\text{-Fe}_2\text{O}_3$ ($10 \text{ m}^2 \text{ l}^{-1}$), pH 5.8; (3) $\gamma\text{-Fe}_2\text{O}_3$ ($8 \text{ m}^2 \text{ l}^{-1}$), pH 4.5; and (4) MnO_2 ($20 \text{ m}^2 \text{ l}^{-1}$), pH 4.9.

corded on an MK II VG Scientific electrostatic spectrometer [$\text{AlK}_{\alpha 7}$ exciting radiation (1486.6 eV)] in a vacuum (10^{-7} Pa) at room temperature [25].

RESULTS AND DISCUSSION

Sorption Kinetics

We found that the time of establishment of the dynamic sorption equilibrium for Pu and Np is influenced by the redox reactions during sorption and by the diffusion to micropores of the sorbent. For example, in sorption of Pu(V) at $\text{pH } 5.0 \pm 0.5$ on MnO_2 and goethite, i.e., when redox reactions can occur [10, 12, 14], the dynamic equilibrium is established in several hours, while in the case of hematite and maghemite [no redox reactions of Pu(V)], this time increases to more than 300 h (Fig. 2). In studying the sorption of U(VI)O_2^{2+} on synthetic goethite, amorphous hydrous Fe oxide, hematite, and on natural hematite, Hsi and Langmuir [26] have demonstrated that the dynamic sorption equilibrium is established in 4 h for

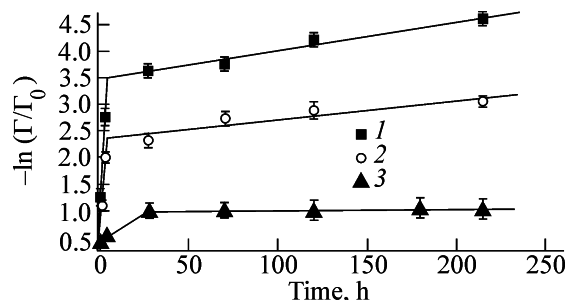


Fig. 3. Sorption kinetics of Np(V) [$c(\text{Np}) = 1.5 \times 10^{-7}$ M, $c(\text{NaClO}_4) = 0.1$ M] on MnO_2 ($55 \text{ m}^2 \text{ l}^{-1}$). pH: (1) 6.0 ± 0.1 , (2) 4.0 ± 0.1 , and (3) 2.0 ± 0.1 .

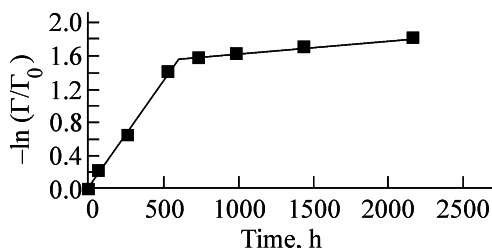


Fig. 4. Sorption kinetics of Pu(V) on hematite ($10 \text{ m}^2 \text{ l}^{-1}$) [$c(\text{Pu}) = 1.8 \times 10^{-8}$ M, $c(\text{NaClO}_4) = 0.1$ M, pH 5.8 ± 0.1].

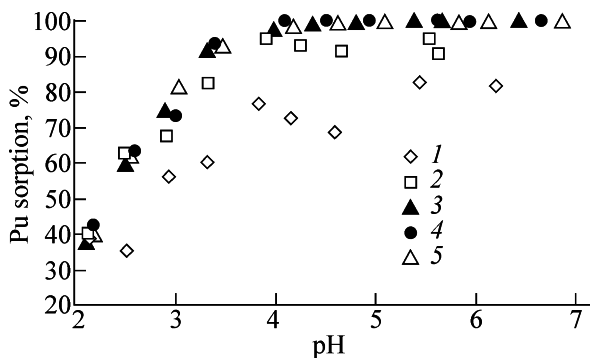


Fig. 5. Sorption from Pu(IV) solution on MnO_2 ($55 \text{ m}^2 \text{ l}^{-1}$) as a function of pH [$c(\text{Pu}) = 5.9 \times 10^{-12}$ M, $c(\text{NaClO}_4) = 0.1$ M] at various sorption times (h): (1) 0.5, (2) 2.5, (3) 25, (4) 49, and (5) 120.

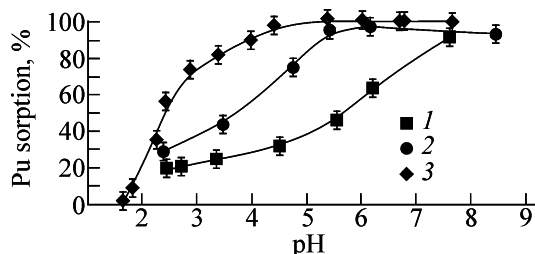


Fig. 6. Sorption from Pu(V) solution on $\alpha\text{-FeOOH}$ ($10 \text{ m}^2 \text{ l}^{-1}$) as a function of pH [$c(\text{Pu}) = 4 \times 10^{-9}$ M, $c(\text{NaClO}_4) = 0.1$ M] at various sorption times (days): (1) 1, (2) 3, and (3) 5 (equilibrium).

$\alpha\text{-FeOOH}$ and $\text{Fe}(\text{OH})_3(\text{amorph.})$ and in 3 days for $\alpha\text{-Fe}_2\text{O}_3$.

The sorption of Np(V), Pu(V), and Pu(IV) proved to proceed in two stages. The fast stage involves the sorption on the outer surface of the sorbents, and the slow stage, diffusion to the micropores (Figs. 3 and 4). Similar results were obtained in [26–28] for the metal sorption on minerals. From the published data on the sorption kinetics of NpO_2^+ on low-crystalline Fe oxide [16], we estimated the diffusion coefficient of Np ($D_s = 2.0 \times 10^{-13} \text{ cm}^2 \text{ s}^{-1}$), and found that the sorption proceeds in two stages, the primary dynamic equilibrium being established in less than an hour.

In all the systems studied, the sorption rate was pH-dependent. In sorption of Pu(IV) on MnO_2 from neutral solutions, the equilibrium is established slightly more slowly as compared to acidic solutions (Fig. 5). In sorption of Pu(V) on $\alpha\text{-FeOOH}$, the sorption rate increases with increasing pH (Fig. 6). Powell et al. [12] reported that, in sorption of Pu(V) on goethite at pH 8, the maximal sorption (>90%) is reached in 30 min, while at pH 6, in 400 min. The authors also indicated that sorption of Pu(V) on synthetic hematite was slower than on goethite.

With increasing Pu(V) concentration by three orders of magnitude (from 10^{-10} to 10^{-7} M), the time of establishment of the dynamic equilibrium of sorption on maghemite increases, indirectly suggesting the effect of diffusion of radionuclides to micro- and mesopores. Similar results were also reported in [15] for sorption of Pu(V) on MnO_2 from deionized water. The authors have found that, with decreasing Pu(V) concentration from 10^{-7} to 10^{-10} M, the sorption of Pu increased from 14 to 40% at a sorption time of 2 h, the time of attainment of the maximal sorption changing insignificantly.

Sorption of Pu(IV)

Figure 7 shows the sorption of Pu(IV) on $\alpha\text{-FeOOH}$, $\alpha\text{-Fe}_2\text{O}_3$, $\gamma\text{-Fe}_2\text{O}_3$, and MnO_2 as influenced by pH. The sorption curve on MnO_2 is shifted to the range of acidic solutions against the other sorbents.

The sorption of trace amounts of Pu(IV) on MnO_2 from 0.1 M NaClO_4 was found to be accompanied by slow oxidation to Pu(VI), whereas in the sorption on the Fe(III) colloids, no change in the Pu(IV) oxidation state was observed. Similar result was obtained by Morgenstern and Choppin [14] for Pu(IV) sorption on MnO_2 at pH 8.1. They have demonstrated that, with increasing concentration of the solid phase in

the solution, the oxidation rate of Pu increases. This is consistent also with data of [9] on oxidation of Pu(V) to Pu(VI) in sorption on mixed-valence Mn oxide, ranseite $(\text{Ca}, \text{Mn}^{\text{II}})\text{O} \cdot 4\text{Mn}^{\text{IV}}\text{O}_2$.

Sorption of Np(V) and Pu(V)

The pH dependences of the sorption of Np(V) and Pu(V) from 0.1 M NaClO_4 are shown in Figs. 8 and 9. The sorption curves of Np on MnO_2 are shifted to the acidic range against those on $\alpha\text{-FeOOH}$, $\alpha\text{-Fe}_2\text{O}_3$, and $\gamma\text{-Fe}_2\text{O}_3$, suggesting tighter binding of Np to MnO_2 . The similar trends are observed for Pu, except for the sorption on $\alpha\text{-FeOOH}$ (in this case, the sorption curve is also shifted to the acidic range). The latter fact indirectly reveals the possibility of occurrence of redox reactions involving Pu(V) in sorption on $\alpha\text{-FeOOH}$.

The liquid extraction data showed that, in sorption on all the investigated colloids, Np(V) changed its oxidation state neither in the solution nor on the sorbent surface. In sorption on $\alpha\text{-FeOOH}$, Pu(V) retained its oxidation state in the solution, being reduced to Pu(IV) on the sorbent surface. Figure 6 shows the sorption of Pu(V) on goethite as influenced by pH. With time, the sorption curve drifts toward lower pH values, which can be considered as an indirect evidence in favor of a slow change in the Pu oxidation state. In sorption of Pu(V) on hematite and maghemite, the initial oxidation state did not change. The results obtained by solvent extraction were confirmed by the XPS spectra. It was demonstrated that Np(V) retained its initial oxidation state during sorption. As for the samples with adsorbed Pu [initially Pu(V)], we found that it was reduced to Pu(IV) on the surface of $\alpha\text{-FeOOH}$. The XPS experiments are described in more detail in our previous paper [25]. Similar results were reported in [12]. However, the mechanism of Pu(V) reduction on goethite and hematite remains to be understood. We observed the reduction of Pu(V) to Pu(IV) on hematite also, but at a considerably lower rate than on goethite. We have not established the mechanism of Pu(V) reduction, but suggested that this reaction could be caused by trace amounts of Fe(II) occurring in the investigated Fe oxides. Another suggestion is that both hematite and goethite, being semiconductors, can carry electrons, thus affecting the Pu oxidation state.

Sorption of Np and Pu as Influenced by Ionic Strength

The results obtained in the sorption experiments at various ionic strengths [$c(\text{NaClO}_4) = 0.01\text{--}0.5$ M]

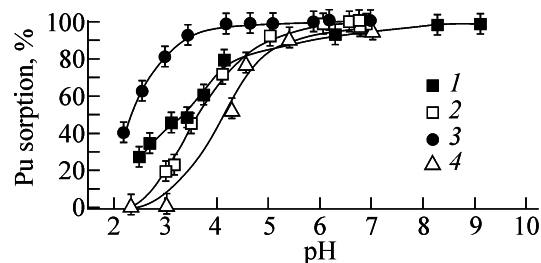


Fig. 7. Sorption from Pu(IV) solutions on (1) $\alpha\text{-FeOOH}$ ($15 \text{ m}^2 \text{ l}^{-1}$), (2) $\gamma\text{-Fe}_2\text{O}_3$ ($10 \text{ m}^2 \text{ l}^{-1}$), (3) MnO_2 ($55 \text{ m}^2 \text{ l}^{-1}$), and (4) $\alpha\text{-Fe}_2\text{O}_3$ ($10 \text{ m}^2 \text{ l}^{-1}$) as a function of pH [$c(\text{NaClO}_4) = 0.1$ M] at various Pu concentrations (M): (1) 1.2×10^{-11} , (2) 6.4×10^{-12} , (3) 5.9×10^{-12} , and (4) 9.3×10^{-10} .

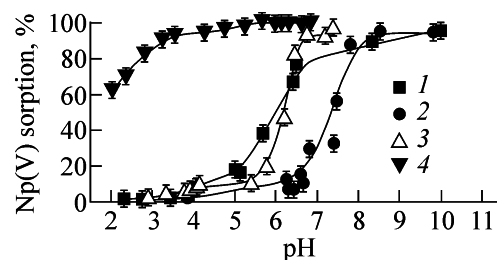


Fig. 8. Sorption of Np(V) on (1) $\alpha\text{-FeOOH}$ ($15 \text{ m}^2 \text{ l}^{-1}$), (2) $\alpha\text{-Fe}_2\text{O}_3$ ($10 \text{ m}^2 \text{ l}^{-1}$), (3) $\gamma\text{-Fe}_2\text{O}_3$ ($10 \text{ m}^2 \text{ l}^{-1}$), and (4) MnO_2 ($55 \text{ m}^2 \text{ l}^{-1}$) as a function of pH [$c(\text{NaClO}_4) = 0.1$ M] at various Np concentrations (M): (1, 2) 7×10^{-7} , (3) 3×10^{-7} , and (4) 1.5×10^{-7} .

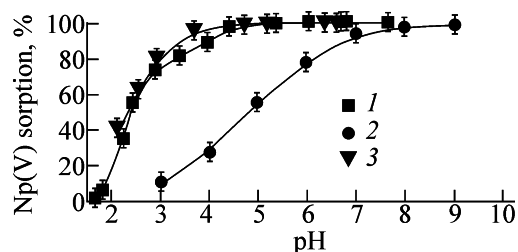


Fig. 9. Sorption from Pu(V) solutions on (1) $\alpha\text{-FeOOH}$ ($15 \text{ m}^2 \text{ l}^{-1}$), (2) $\alpha\text{-Fe}_2\text{O}_3$ ($10 \text{ m}^2 \text{ l}^{-1}$), and (3) MnO_2 ($55 \text{ m}^2 \text{ l}^{-1}$) as a function of pH [$c(\text{NaClO}_4) = 0.1$ M] at various Pu concentrations (M): (1, 3) 1.8×10^{-8} and (2) 2×10^{-8} .

showed that the ionic strength has no effect on the sorption curves of Np(V), Pu(V), and Pu(IV), suggesting that inner-sphere complexes are formed on the colloid surface [29].

Equilibrium Constants of the Sorption Reactions

Using FITEQL program pack [3], based on Gibbs energy minimization, we have found that the diffusion layer model is best suited to reproduce our experi-

Table 2. Stability constants of surface complexes of actinides adsorbed on colloids, as estimated by FITEQL

Phase	Reaction	log K
α -FeOOH	$\sim\text{Fe-OH} + \text{NpO}_2^+ \rightleftharpoons \sim\text{Fe-O-NpO}_2 + \text{H}^+$	-1.41
α -FeOOH	$\sim\text{Fe-OH} + \text{Pu}^{4+} \rightleftharpoons \sim\text{Fe-O-Pu}^{3+} + \text{H}^+$	2.64
α -FeOOH	$\sim\text{Fe-OH} + \text{Pu}^{4+} + \text{H}_2\text{O} \rightleftharpoons \sim\text{Fe-O-Pu(OH)}^{2+} + 2\text{H}^+$	-1.93
α -FeOOH	$\sim\text{Fe-OH} + \text{Pu}^{4+} + 2\text{H}_2\text{O} \rightleftharpoons \sim\text{Fe-O-Pu(OH)}_2^+ + 3\text{H}^+$	-5.87
α -FeOOH	$\sim\text{Fe-OH} + \text{Pu}^{4+} + 3\text{H}_2\text{O} \rightleftharpoons \sim\text{Fe-O-Pu(OH)}_3 + 4\text{H}^+$	-11.9
α -Fe ₂ O ₃	$\sim\text{Fe-OH} + \text{NpO}_2^+ \rightleftharpoons \sim\text{Fe-O-NpO}_2 + \text{H}^+$	-2.12
α -Fe ₂ O ₃	$\sim\text{Fe-OH} + \text{PuO}_2^+ \rightleftharpoons \sim\text{Fe-O-PuO}_2 + \text{H}^+$	-2.14
γ -Fe ₂ O ₃	$\sim\text{Fe-OH} + \text{NpO}_2^+ \rightleftharpoons \sim\text{Fe-O-NpO}_2 + \text{H}^+$	-2.49
γ -Fe ₂ O ₃	$\sim\text{Fe-OH} + \text{NpO}_2^+ \rightleftharpoons \sim\text{Fe-O-PuO}_2 + \text{H}^+$	-2.37
MnO ₂	$\sim\text{Mn-OH} + \text{NpO}_2^+ \rightleftharpoons \sim\text{Mn-O-NpO}_2 + \text{H}^+$	0.25

Note: Tilde denotes the surface of colloid particles.

mental data on actinide sorption on the colloidal oxides. All the possible complexation reactions were included in calculation, but the formation of monodentate actinide complexes was found to be the most probable. We estimated the stability constants of the Np(V) complexes formed in sorption on all the oxides studied, those of Pu(IV) on goethite, and of Pu(V) on hematite and maghemite (Table 2). For Np, the equilibrium constants decrease in the order $K_{\text{MnO}_2} > K_{\alpha\text{-FeOOH}} > K_{\alpha\text{-Fe}_2\text{O}_3} \sim K_{\gamma\text{-Fe}_2\text{O}_3}$. Therefore, the behavior of actinides in the environment is controlled to a considerable extent by the sorption on Mn oxides. Data on the equilibrium constants may be used for estimation of the distribution coefficients in the actual underground water–colloid systems.

The stability constants of the complexes $\sim\text{Fe-O-NpO}_2$, obtained in this study for goethite and hematite, are well consistent with those reported by Kohler et al. [18] ($\log K = -1.565$ and -2.090 , respectively).

ACKNOWLEDGMENTS

The study was financially supported by the DOE–RAS Joint Program (project RUC2-20008-MO-04) and Russian Foundation for Basic Research (project 05-03-33028).

REFERENCES

- Kim, J.I., *Radiochim. Acta*, 1991, vol. 52, no. 3, pp. 71–81.
- Kim, J.I., Buckau, G., and Klenze, R., *Natural Analogues in Radioactive Waste Disposal*, Come, B. and Chapman, N.A., Eds., Graham & Trotman, 1987, pp. 289–299.
- Novikov, A.P. and Myasoedov, B.F., *Environment Protection against Radioactive Pollution*, Birsen, N. and Kadyrzhanov, K.K., Eds., Kluwer, 2003, pp. 147–154.
- McCarthy, J.F. and Zachara, Z.M., *Environ. Sci. Technol.*, 1989, vol. 23, pp. 496–502.
- Clark, S.B., Johnson, W.H., Malek, M.A., et al., *Radiochim. Acta*, 1996, vol. 74, pp. 173–179.
- Myasoedov, B.F. and Novikov, A.P., *J. Radioanal. Nucl. Chem.*, 1998, vol. 229, pp. 33–38.
- Kersting, A.B., Efurud, D.W., Finnegan, D.L., et al., *Nature*, 1999, vol. 396, no. 6714, pp. 56–59.
- Penrose, W.R., Polzer, W.L., Essington, E.H., et al., *Environ. Sci. Technol.*, 1990, vol. 24, no. 2, pp. 228–234.
- Duff, M.C., Hunter, D.B., and Triay, I.R., *Environ. Sci. Technol.* 1999, vol. 33, pp. 2163–2169.
- Sanchez, A.L., Murray, J.W., Sibley, T.H., et al., *Geochim. Cosmochim. Acta*, 1985, vol. 49, pp. 2297–2307.
- Waite, T.D., Davis, J.A., Payne, T.E., et al., *Geochim. Cosmochim. Acta*, 1994, vol. 58, no. 24, pp. 5465–5478.
- Powell, B.A., Fjeld, R.A., Kaplan, D.I., et al., *Environ. Sci. Technol.*, 2005, vol. 39, no. 7, pp. 2107–2114.
- Shaughnessy, D., Nitshe, H., and Shuh, D., *J. Nucl. Sci. Technol.*, 2002, suppl. 3, pp. 274–277.
- Morgenstern, A. and Choppin, G.R., *Radiochim. Acta*, 2002, vol. 90, pp. 69–74.
- Keeney-Kennicutt, W.L. and Morse, J.W., *Geochim. Cosmochim. Acta*, 1985, vol. 49, pp. 2577–2588.

16. Nagasaki, Sh., Tanaka, S., Todoriki, M., and Suzuki, A., *J. Alloys Comp.*, 1998, vol. 271, pp. 252–256.
17. Sapiieszko, R.S. and Matijevic, E., *J. Colloid Interface Sci.*, 1980, vol. 74, no. 2, pp. 405–422.
18. Kohler, M., Honeyman, B.D., and Leckie, J.O., *Radiochim. Acta.*, 1999, vol. 85, pp. 33–48.
19. Atkinson, R.J., Posner, A.M., and Quirk, J.P., *J. Phys. Chem.*, 1967, vol. 71, no. 3, pp. 550–558.
20. Penners, N.H.G. and Koopal, L.K., *Colloids Surf.*, 1986, vol. 19, pp. 337–349.
21. Herrero, E., Cabanas, M.V., Vallet-Regi, M., et al., *Solid State Ionics*, 1997, vols. 101–103, no. 1, pp. 213–219.
22. Murray, J.W., *J. Colloid Interface Sci.*, 1974, vol. 46, pp. 357–371.
23. Nesmeyanov, An.N., *Rukovodstvo k prakticheskim zanyatiyam po radiokhimii* (Practical Course of Radiochemistry), Moscow: Khimiya, 1968, pp. 458–465.
24. Choppin, G.R., *J. Radioanal. Nucl. Chem.*, 1990, vol. 147, no. 1, pp. 109–116.
25. Teterin, Yu.A., Kalmykov, S.N., Novikov, A.P., et al., *Radiokhimiya*, 2004, vol. 46, no. 6, pp. 545–552.
26. Hsi, Ch.D. and Langmuir, D., *Geochim. Cosmochim. Acta*, 1985, vol. 45, pp. 1931–1941.
27. Davis, J.A. and Kent, D.B., *Rev. Mineral.*, 1990, vol. 23, pp. 177–260.
28. Axe, L. and Anderson, P.R., *J. Colloid Interface Sci.*, 1995, vol. 175, pp. 157–165.
29. Payne, T.E., *PhD Thesis*, Univ. of New South Wales, 1999.
30. Herbelin, A.L. and Kent, D.B., *FITEQL: A Computer Program for Determination of Equilibrium Constants from Experimental Data, ver. 3.1*, Corvallis: Department of Chemistry, Oregon State Univ., 1994, Report 94-01.